

Emerging Microbes & Infections

ISSN: 2222-1751 (Online) Journal homepage: www.tandfonline.com/journals/temi20

OXA-48-like carbapenemases in *Proteus mirabilis* – novel genetic environments and a challenge for detection

Janko Sattler, Janina Noster, Yvonne Stelzer, Martina Spille, Sina Schäfer, Kyriaki Xanthopoulou, Julian Sommer, Jonathan Jantsch, Silke Peter, Stephan Göttig, Sören G. Gatermann & Axel Hamprecht

To cite this article: Janko Sattler, Janina Noster, Yvonne Stelzer, Martina Spille, Sina Schäfer, Kyriaki Xanthopoulou, Julian Sommer, Jonathan Jantsch, Silke Peter, Stephan Göttig, Sören G. Gatermann & Axel Hamprecht (2024) OXA-48-like carbapenemases in *Proteus mirabilis* – novel genetic environments and a challenge for detection, Emerging Microbes & Infections, 13:1, 2353310, DOI: 10.1080/22221751.2024.2353310

To link to this article: https://doi.org/10.1080/22221751.2024.2353310

© 2024 The Author(s). Published by Informa UK Limited, trading as Taylor & Francis Group, on behalf of Shanghai Shangyixun Cultural Communication Co., Ltd

View supplementary material

Published online: 23 May 2024.

Submit your article to this journal

Article views: 2639

View related articles

View Crossmark data

Citing articles: 17 View citing articles

Full Terms & Conditions of access and use can be found at
https://www.tandfonline.com/action/journalInformation?journalCode=temi20

Emerging Microbes & Infections
2024, VOL. 13, 2353310 (12 pages)
https://doi.org/10.1080/22221751.2024.2353310

OPEN ACCESS Check for updates

OXA-48-like carbapenemases in *Proteus mirabilis* – novel genetic environments and a challenge for detection

Janko Sattler [a,b,f], Janina Noster [b], Yvonne Stelzer[b], Martina Spille[b], Sina Schäfer[a,f], Kyriaki Xanthopoulou [a,f], Julian Sommer [d], Jonathan Jantsch[a,f], Silke Peter[c,f], Stephan Göttig [d], Sören G. Gatermann[e] and Axel Hamprecht [a,b,f]

[a]Institute for Medical Microbiology, Immunology and Hygiene, University Hospital Cologne and Faculty of Medicine, University of Cologne, Cologne, Germany; [b]Institute for Medical Microbiology and Virology, University of Oldenburg, Oldenburg, Germany; [c]Institute of Medical Microbiology and Hygiene, University Hospital Tuebingen, Tuebingen, Germany; [d]Goethe University Frankfurt, University Hospital, Institute of Medical Microbiology and Infection Control, Frankfurt am Main, Germany; [e]National Reference Laboratory for Multidrug-Resistant Gram-negative Bacteria, Department of Medical Microbiology, Ruhr-University Bochum, Bochum, Germany; [f]German Centre for Infection Research (DZIF)

ABSTRACT

OXA-48-like enzymes represent the most frequently detected carbapenemases in Enterobacterales in Western Europe, North Africa and the Middle East. In contrast to other species, the presence of OXA-48-like in *Proteus mirabilis* leads to an unusually susceptible phenotype with low MICs for carbapenems and piperacillin-tazobactam, which is easily missed in the diagnostic laboratory. So far, there is little data available on the genetic environments of the corresponding genes, $bla_{\text{OXA-48}}$-like, in *P. mirabilis*. In this study susceptibility phenotypes and genomic data of 13 OXA-48-like-producing *P. mirabilis* were investigated (OXA-48, $n = 9$; OXA-181, $n = 3$; OXA-162, $n = 1$). Ten isolates were susceptible to meropenem and ertapenem and three isolates were susceptible to piperacillin-tazobactam. The gene $bla_{\text{OXA-48}}$ was chromosomally located in 7/9 isolates. Thereof, in three isolates $bla_{\text{OXA-48}}$ was inserted into a *P. mirabilis* genomic island. Of the three isolates harbouring $bla_{\text{OXA-181}}$ one was located on an IncX3 plasmid and two were located on a novel MOB_{F} plasmid, pOXA-P12, within the new transposon Tn*7713*. In 5/6 isolates with plasmidic location of $bla_{\text{OXA-48}}$-like, the plasmids could conjugate to *E. coli* recipients *in vitro*. *Vice versa*, $bla_{\text{OXA-48}}$-carrying plasmids could conjugate from other Enterobacterales into a *P. mirabilis* recipient. These data show a high diversity of $bla_{\text{OXA-48}}$-like genetic environments compared to other Enterobacterales, where genetic environments are quite homogenous. Given the difficult-to-detect phenotype of OXA-48-like-producing *P. mirabilis* and the location of $bla_{\text{OXA-48}}$-like on mobile genetic elements, it is likely that OXA-48-like-producing *P. mirabilis* can disseminate, escape most surveillance systems, and contribute to a hidden spread of OXA-48-like.

ARTICLE HISTORY Received 1 January 2024; Revised 14 April 2024; Accepted 5 May 2024

KEYWORDS *Proteus mirabilis*; OXA-48; OXA-181; OXA-162; carbapenemase-producing Enterobacterales

Introduction

Carbapenemases are important mediators of multidrug resistance in Enterobacterales. They can render bacteria resistant to carbapenems and most other β-lactam antibiotics. The most frequently detected carbapenemase type in Enterobacterales in Western Europe, North Africa, and the Middle East are OXA-48-like carbapenemases [1]. This group encompasses OXA-48 and variants of the latter with minor changes in the amino acid sequence, e.g. OXA-181 and OXA-162. OXA-48-like are most often reported in *Klebsiella pneumoniae*, *Escherichia coli* and the *Enterobacter cloacae* complex, but much less frequently in other Enterobacterales [2]. Especially in *Proteus mirabilis*, OXA-48-like carbapenemases have only been rarely described [3]. Interestingly, some of the reported isolates exhibited low minimum inhibitory concentrations (MICs) for piperacillin-tazobactam (PIT) [4,5], which is a particularity in carbapenemase-producing Enterobacterales (CPE). OXA-48-like enzymes have only weak hydrolytic activity against carbapenems *in vitro*, which results in low MIC values if no other resistance mechanism is present. The combination of low MIC values for carbapenems and PIT strongly impedes the detection of OXA-48-like-producing *P. mirabilis* in the diagnostic laboratory, since these parameters are often included in diagnostic algorithms for the detection of carbapenemases [6,7]. Nevertheless, the detection of OXA-48-like is crucial, as it has been shown that carbapenems are not an

CONTACT Janko Sattler jankosattler@gmail.com Institute for Medical Microbiology, Immunology, and Hygiene, University Hospital Cologne, Goldenfelsstr. 19 -21, Cologne 50935, Germany

Supplemental data for this article can be accessed online at https://doi.org/10.1080/22221751.2024.2353310.

© 2024 The Author(s). Published by Informa UK Limited, trading as Taylor & Francis Group, on behalf of Shanghai Shangyixun Cultural Communication Co., Ltd
This is an Open Access article distributed under the terms of the Creative Commons Attribution License (http://creativecommons.org/licenses/by/4.0/), which permits unrestricted use, distribution, and reproduction in any medium, provided the original work is properly cited. The terms on which this article has been published allow the posting of the Accepted Manuscript in a repository by the author(s) or with their consent.

effective treatment option for OXA-48-producing Enterobacterales even if they have MICs within the susceptible range [8]. As *P. mirabilis* is intrinsically resistant to colistin and tigecycline, the choice of last-resort antibiotics is limited in infections with these isolates.

Compared to other carbapenemase genes, the genomic location of $bla_{\text{OXA-48}}$, the gene coding for OXA-48, is quite homogenous in Enterobacterales. The most common genomic location is on ~60-70 kb sized IncL plasmids [9] which represent variants of the originally described pOXA-48 [10]. Within these plasmids, $bla_{\text{OXA-48}}$ is located on variants of the transposon Tn*1999* of which eight have been described until now [11]. However, from the little data published, the genetic environment of $bla_{\text{OXA-48}}$ in *P. mirabilis* was either located on an unusually large IncL/M plasmid [12] or integrated into the host chromosome [4]. This raises doubts if genomic findings on $bla_{\text{OXA-48}}$ in other Enterobacterales can be applied to OXA-48-producing *P. mirabilis*.

It is, therefore, unclear whether the low PIT MICs observed in some OXA-48-like-producing *P. mirabilis* isolates are associated with a particular genomic configuration of $bla_{\text{OXA-48}}$-like-associated environments. Additionally, it is unknown if $bla_{\text{OXA-48}}$-like are usually located on mobile genetic elements in *P. mirabilis*, and could serve as a hidden source for the spread of $bla_{\text{OXA-48}}$-like to other Enterobacterales, as postulated very recently [4,5]. In this study, we aim to analyse the genetic environments and transferability of $bla_{\text{OXA-48}}$-like genes in clinical *P. mirabilis* isolates, together with their susceptibility phenotypes.

Methods

Isolates and antibiotic susceptibility testing

Thirteen OXA-48-like-producing *P. mirabilis* isolates from clinical samples were included in the study. They were collected between 2015 and 2021 at the University Hospital Cologne, the University Hospital Frankfurt am Main and the German National Reference Centre for multidrug-resistant Gram-negative bacteria Bochum, including twelve isolates from Germany and one isolate from Austria. The presence of OXA-48-like was confirmed by lateral flow test (RESIST-4 O.K.N.V., Coris BioConcept, Gembloux, Belgium) [13] and PCR (GeneXpert Carba-R assay, Cepheid, Frankfurt, Germany) [14]. Minimal inhibitory concentrations for ertapenem, meropenem, and PIT were determined using broth microdilution (BMD; Micronaut-S, Merlin, Bornheim, Germany). When MICs were outside of the dilution steps of BMD, gradient tests (MIC strips, Liofilchem, Roseto degli Abruzzi, Italy) were used to determine the values. Samples were tested in triplicates and the median MIC value per isolate and antibiotic was reported. The MICs were interpreted for susceptibility according to EUCAST clinical breakpoints version 13.1. To compare MIC values between two isolate groups, the Mann–Whitney test was used and a p-value ≤ 0.05 considered statistically significant.

In vitro plasmid conjugation

Horizontal gene transfer via conjugation was conducted by liquid mating assay as described before [11]. From *P. mirabilis* donors with $bla_{\text{OXA-48}}$ located on plasmids, conjugation was evaluated employing the sodium azide-resistant acceptor strain *E. coli* J53 and *K. pneumoniae* PRZ. *Vice versa*, conjugation of isogenic $bla_{\text{OXA-48}}$-carrying plasmids from clinical non-*Proteus* Enterobacterales isolates was performed in parallel into acceptor strains J53 and a sodium azide-resistant *P. mirabilis* strain, further referred to as ARP. Successful conjugation was confirmed by antibiotic susceptibility testing, MALDI-TOF, and whole genome sequencing (WGS). Quantitative conjugation was conducted in three independent runs and the mean conjugation rate and standard deviation was reported.

Genetic analysis

For genetic analysis, DNA was extracted from pure bacterial cultures using the DNeasy UltraClean Microbial Kit (Qiagen, Hilden, Germany). Whole genome sequencing was performed with short- and long-read sequencing technology. Briefly, libraries were prepared with the native barcoding kits SQK-LSK109 or SQK-NBD114 (Oxford Nanopore Technologies, Oxford, UK), and Illumina DNA Prep (Illumina, San Diego, CA, United States) and sequencing was performed on a Oxford Nanopore PromethION with flow cell type R9.4.1 or R10.4.1 and on a Illumina NextSeq500. Genomes were assembled from long-reads with Trycycler [15] followed by long-read polishing with medaka [16] and short-read polishing with polypolish [17]. The classes and abundances of resistance genes and plasmids were determined using the ResFinder and PlasmidFinder databases [18,19]. Plasmids that could not be classified by PlasmidFinder were further characterized using MOBscan [20] and MOB-suite [21]. Sequences were annotated using the automated PGAP pipeline of NCBI [22], as well as manually. For the phylogenetic analysis all publicly available sequences of OXA-48-like-producing *P. mirabilis* from GenBank were included. A cgMLST scheme was created with chewBBACA [23]. Allele calling was performed with a threshold of 95% loci presence in the test dataset, resulting in 2,334 loci. A minimum spanning tree was created from the allelic profiles using GrapeTree [24]. For isolates of

the same ST type, whole genome SNP analysis was performed with CSIPhylogeny 1.4 [25]. The GenBank accession numbers of external isolates included in the phylogenetic analysis are shown in Supplementary Table 1. Comparative genome graphs were created with BRIG 0.95 [26] and clinker [27].

Data availability

The complete nucleotide sequence assemblies of all OXA-48-like-producing *P. mirabilis* were deposited at DDBJ/ENA/GenBank under BioProject no. PRJNA982542. Accession numbers are listed in Supplementary Table 2.

Ethics

Due to the retrospective design of this study which involved only bacterial isolates, no approval by an ethics committee is required according to § 15 of the professional code for physicians of North Rhine-Westphalia. This was confirmed by the ethics committee of the University Hospital Cologne under the statement number "23-1212-retro".

Results

Isolates and antibiotic susceptibility testing

Of the 13 isolates included in this study, nine produced OXA-48, three OXA-181, and one OXA-162 (Table 1). For most isolates, ertapenem and meropenem MICs were between 0.25 and 1 mg/L; 10/13 isolates (77%) were susceptible to ertapenem, and 11/13 (85%) to meropenem. Exceptionally, P1, P12, and P13 showed elevated MICs for meropenem and/or ertapenem. MICs for PIT were >64 mg/L in 8/13 isolates (62%), while MICs in the susceptible range (≤ 8 mg/L) were recorded in three isolates (P1, P4, and P5).

Phylogeny

A minimum spanning tree was created for allelic differences in the cgMLST, including all isolates from this study ($n = 13$) and non-redundant publicly available sequences on GenBank of OXA-48-like-producing *P. mirabilis* ($n = 43$) (Figure 1). While most isolates were only distantly related, some isolates formed small clusters within the same ST type. Amongst these, P1 and P6 (ST479) showed no allelic difference and only 11 SNPs difference in the whole genome and were isolated from adjacent geographical regions (Rhine-Main area), about one month apart, making an epidemiological relationship likely. The other clusters were P12 and P13 (ST446, 26 allelic and 55 SNP difference), P3, P8 and the external isolates NY1 and WA1 (ST135, 83–122 allelic and 646–1050 SNP differences) and P10 and AUS1 (ST178, 132 allelic and 731 SNP differences). They showed no close regional and temporal context.

Table 1. Genotypic and phenotypic characteristics of OXA-48-like-producing *P. mirabilis* isolates from this study.

Isolate	Isolation date	Isolation place	OXA-48 type	Genomic location of bla_{OXA-48}-like	Plasmid size (bp)	Additional plasmids (bp)	Other β-lactamases	Genetic environment	MIC		
									ERT	MER	PIT
P1	11/2016	Main-Kinzig-Kreis (Hesse)	OXA-48	chromosomal	–	–	CTX-M-14b	Δ1_pOXA-48-PM	4	8	4
P2	04/2017	Munich (Bavaria)	OXA-48	chromosomal	–	–	TEM-1B	Tn*6237*	0.5	0.5	64
P3	08/2017	Esslingen (Baden-Württemberg)	OXA-48	chromosomal	–	40,918 (MOB_P) 26,817 (MOB_C)	CTX-M-14b, TEM-1B, TEM-2	Δ3_pOXA-48-PM	0.5	1	32
P4	02/2020	Barnim (Brandenburg)	OXA-48	chromosomal	–	37,771 (MOB_P) 37,694	CTX-M-14b, TEM-1B	Δ4_pOXA-48-PM	0.25	0.25	4
P5	01/2021	Recklinghausen (North Rhine-Westphalia)	OXA-48	chromosomal	–	–	–	Tn*6237*	0.5	0.5	4
P6	10/2016	Frankfurt am Main (Hesse)	OXA-48	chromosomal	–	–	CTX-M-14b	Δ1_pOXA-48-PM	0.5	1	>64
P7	08/2018	Cologne (North Rhine-Westphalia)	OXA-48	chromosomal	–	–	–	Tn*6237*	0.25	0.5	64
P8	09/2019	Mainz (Rhineland Palatinate)	OXA-48	IncL plasmid	63,589	36,059 (MOB_P) 2,089 (Col)	CTX-M-65, TEM-1B, OXA-1	invTn*1999.2*	0.25	0.5	32
P9	01/2020	District Saxon Switzerland (Saxony)	OXA-162	IncL plasmid	66,644	–	CTX-M-15	Tn*1999.2*	0.5	1	>64
P10	02/2018	Neuss (North Rhine-Westphalia)	OXA-48	IncM plasmid	141,887	–	CTX-M-14b, OXA-10, CARB-2	Δ2_pOXA-48-PM	0.5	1	>64
P11	02/2020	Linz (Austria)	OXA-181	IncX3 plasmid	51,479	–	–	Tn*6360*-like	0.5	0.5	16
P12	12/2015	Berlin	OXA-181	MOB_F plasmid	49,093	–	VEB-6, TEM-1B	Tn*7713*	1	4	>64
P13	07/2018	Bochum (North Rhine-Westphalia)	OXA-181	MOB_F plasmid	49,093	–	VEB-6, TEM-1B	Tn*7713*	1	2	>64

Note: If plasmids were not typeable by their replication unit, the MOB type was given, if available. Interpretation of MICs according to EUCAST breakpoints is colour encoded; red = resistant; yellow = susceptible, increased exposure; green = susceptible, standard dosing regimen. MIC = minimum inhibitory concentration, ERT = ertapenem, MER = meropenem, PIT = piperacillin-tazobactam. See the online article for the color version of this table.

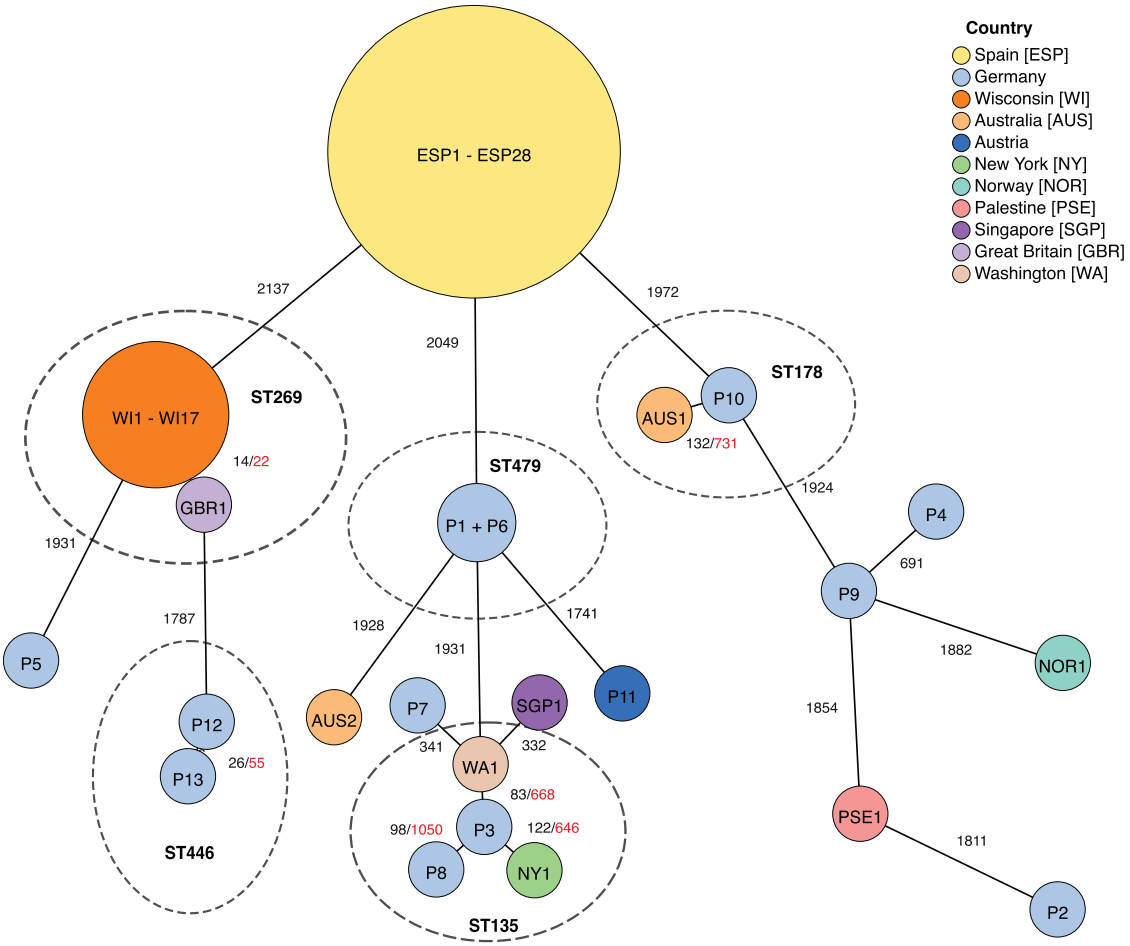

Figure 1. Maximum-likelihood cgMLST-based phylogeny of OXA-48-like-producing *P. mirabilis* from this study and external sequences from GenBank. The distance of the tree branches represents allelic differences in the cgMLST scheme (in total 2,334 loci). Nodes with close epidemiological relationship were combined in one node (cut-off: 12 allelic differences). Isolates with the same ST type are indicated by dotted circles. Within the same ST type, genomic distances are also expressed as SNPs from whole genome phylogeny (red numbers).

Genetic support of bla$_{OXA-48}$-like

In all isolates, the genetic environment of *bla*$_{OXA-48}$-like was examined using hybrid assemblies. In 7/9 OXA-48-producing isolates, *bla*$_{OXA-48}$ was located on the chromosome. In the other two isolates, *bla*$_{OXA-48}$ was located on an IncL or IncM plasmid, respectively. The closely related gene *bla*$_{OXA-162}$ was also situated on an IncL plasmid in one isolate. The gene *bla*$_{OXA-181}$ was located on an IncX3 plasmid in one isolate and a novel MOB$_F$ plasmid in two isolates (Table 1).

Chromosomal location of bla$_{OXA-48}$

In the seven isolates with chromosomal localization, different genetic environments of *bla*$_{OXA-48}$ were observed. In isolates P2, P5, and P7, *bla*$_{OXA-48}$ was integrated via the IS*1R*-bounded composite transposon Tn*6237* (Figure 2). For the other four isolates, the genetic environments of *bla*$_{OXA-48}$ show high sequence homology with different genetic subsections of the plasmid pOXA-48-PM, which was the first *bla*$_{OXA-48}$-carrying plasmid described in *P. mirabilis* [12] (Figure 2). These four genomic regions are therefore referred to as Δ1_pOXA-48-PM to Δ4_pOXA-48-PM.

In isolate P3, Δ3_pOXA-48-PM spans from IS*1R* next to *bla*$_{OXA-48}$ until *strB*, but harbours an additional IS*Pa14*, truncating *mucA*. Isolate P1 and P6 harbour Δ1_pOXA-48-PM, which is a variant of Δ3_pOXA-48-PM missing the additional IS*Pa14* as well as IS*Ecp1* upstream of *bla*$_{CTX-M-14}$ together with two ORFs. Isolate P4 hosts Δ4_pOXA-48-PM, which has its starting point further upstream of the *bla*$_{OXA-48}$-harbouring invTn*1999.2*, spanning the whole pOXA-48-PM region from *ΔrepA* until IS*Ecp1*.

In isolates harbouring Tn*6237* and Δ4_pOXA-48-PM, all genetic environments of *bla*$_{OXA-48}$ were chromosomally integrated into different sites of the conserved genetic region of *P. mirabilis*. For Δ4_pOXA-48-PM the integrated sequence is bounded by 12 bp imperfect inverted repeats containing five mismatches and flanked by 5 bp target site duplications, indicating one-ended transposition by IS*Ecp1* (Figure 2). Tn*6237* was integrated in

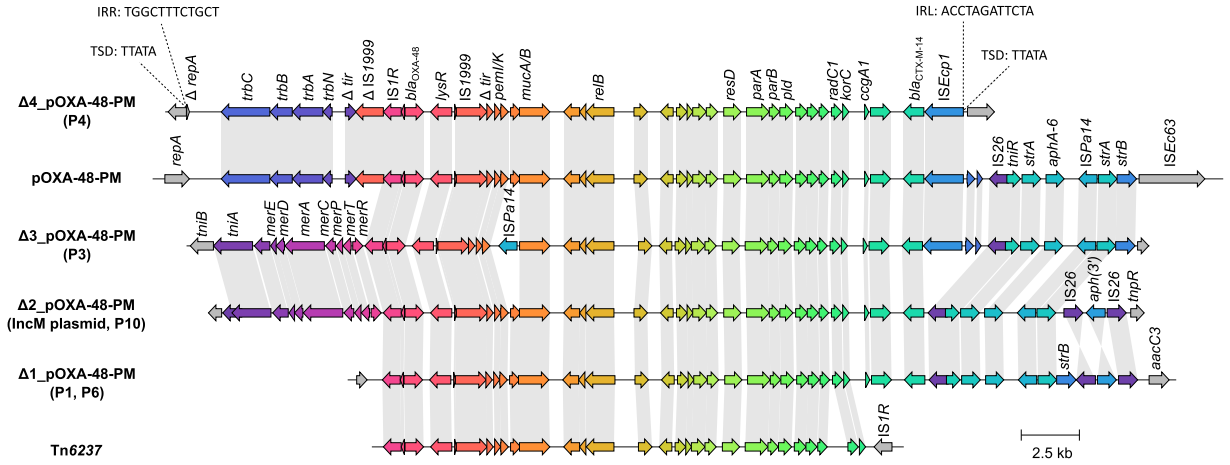

Figure 2. Variants of genetic environments of *bla*$_{OXA-48}$ in *P. mirabilis* compared to the plasmid pOXA-48-PM. Grey arrows indicate mobile genetic elements or associated genes. Unlabelled arrows indicate genes coding for hypothetical proteins. IRL/IRR = left and right inverted repeats. TSD = target site duplications.

different genetic sites in the three isolates, expectedly resulting in different 9 bp sized target site duplications. In contrast, in the other three isolates with chromosomal ΔpOXA-48-PM variants (P1, P3, and P6), the genetic environment of *bla*$_{OXA-48}$ was integrated in novel variants of the genomic island PmGRI1 [28], not flanked by target site duplications. The GC content of the novel genomic islands was 53.2-54.9% compared to 38.9% for the *P. mirabilis* reference strain HI4320. Like PmGRI1, these genomic islands are integrated at the 3′ end of tRNA-Sec in the vicinity of the *prlC* gene and share the same backbone, including complete homology within the integrase gene. Therefore, they are referred to as PmGRI1-P1, -P3, and -P6. PmGRI1-P6 is 96,474 bp in size. Besides the genomic island backbone of PmGRI1 and ΔpOXA-48-PM, it contains sequence regions homologous with parts of the genomic island GIPmi1 (accession number MF490433) (Figure 3). PmGRI1-P1 has a highly similar composition to PmGRI-P1, but an excision in a repetitive region resulted in a smaller size of 77,906 bp. PmGRI1-P3

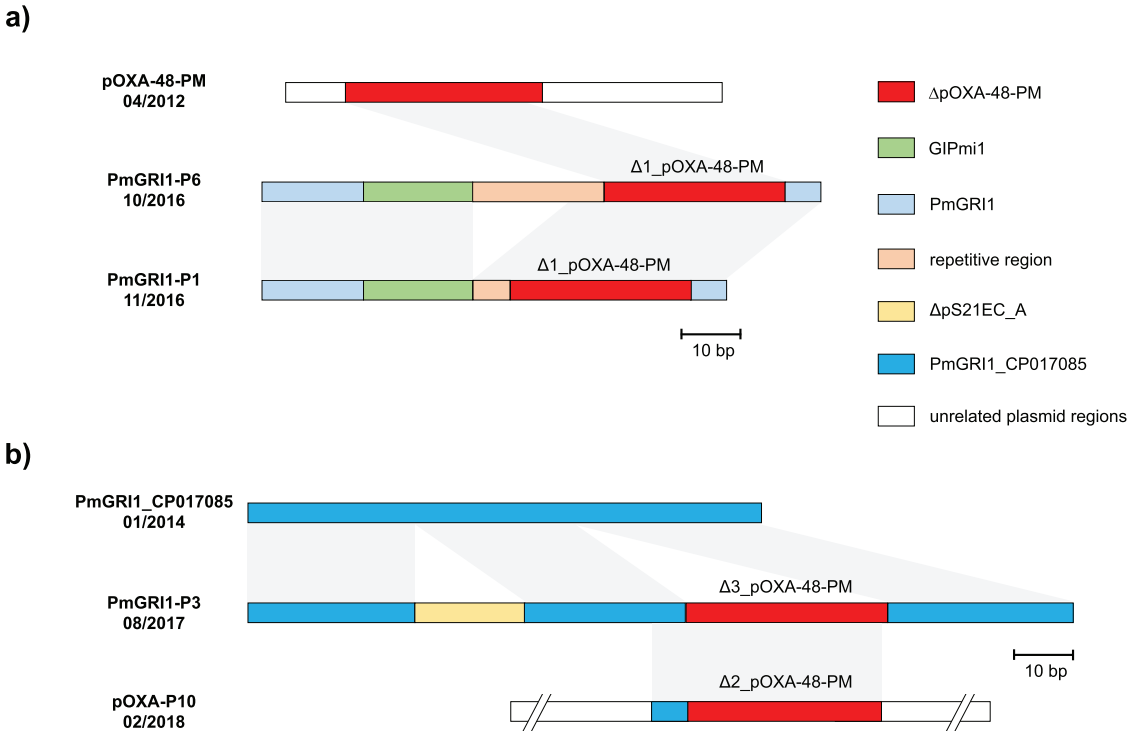

Figure 3. Graphical representation of the novel genomic islands PmGRI1-P1/P6 (a) and PmGRI1-P3 and the plasmid pOXA-P10 (b). Genetic structures are colour encoded according to the legend. Grey areas between the structures indicate regions of high sequence homology. Numbers below the name label describe the isolation date of the according isolate.

shows high sequence homology with a PmGRI1 variant published under the accession number CP017085 [29]. It differs from the latter by the addition of ΔpOXA-48-PM as well as parts of an *E. coli* plasmid, pS21EC_A (accession number CP076690) [30], resulting in a size of 139,172 bp.

Plasmidic location of $bla_{OXA-48/162}$

In P8 and P9, bla_{OXA-48}-like were located on IncL plasmids, further referred to as pOXA-P8 and pOXA-P9. In pOXA-P8, bla_{OXA-48} was located on an inverted Tn*1999.2*, and, compared to the originally described pOXA-48, the plasmid contains an additional IS*1R* element downstream of *korC* (Figure 4). In pOXA-P9, $bla_{OXA-162}$ was located on a Tn*1999.2* transposon. Compared to pOXA-P8, this plasmid harbours an additional 3,049 bp IS*Ecp1* transposition unit carrying $bla_{CTX-M-15}$ as cargo gene, truncating *klcA*. Both IncL plasmids were transferable from their *P. mirabilis* donor to *E. coli* J53 via conjugation and pOXA-P9 was also transferable to *K. pneumoniae* PRZ. The IncM plasmid pOXA-P10 did not conjugate to J53 or PRZ in our *in vitro* assay.

Plasmidic location of $bla_{OXA-181}$

Three isolates harboured $bla_{OXA-181}$. In isolate P11, $bla_{OXA-181}$ was located on a 51,479 bp-sized IncX3 plasmid, further referred to as pOXA-P11. This IncX3 plasmid is identical to plasmids described in other species, e.g. pOXA-181_14828 (accession number KP400525) [31]. In the other two isolates, P12 and P13, $bla_{OXA-181}$ is located on a novel 49,093 bp-sized plasmid, further referred to as pOXA-P12 (Figure 5). This plasmid could not be typed to a known Inc group, but the relaxase gene could be assigned to the MOB_F type. The plasmids of these two isolates show 100% sequence identity, despite being isolated three years apart.

In all three isolates, $bla_{OXA-181}$ was surrounded by a genetic environment related to the Tn*6360* transposon (Figure 6). In pOXA-P11, the genetic environment is identical to that of a Tn*6360* variant described before [31] and is here referred to as Tn*6360*-like. In pOXA-P12, $bla_{OXA-181}$ was found on a novel variant of Tn*6360*-like. This variant is truncated upstream of the ΔTn*3*-like sequence and was assigned the name Tn*7713* by the transposon registry [32] (Figure 6). Tn*7713* is bounded by 14 bp inverted repeats and flanked by 8 bp target site duplications.

Both $bla_{OXA-181}$-carrying plasmid types could conjugate to *E. coli* J53, while only pOXA-P11 conjugated to PRZ. WGS analysis of the transconjugants showed that pOXA-P11 and pOXA-12 stayed intact during the transfer except for one conjugation experiment, where plasmid pOXA-P12 was integrated into the chromosome of the recipient J53, bounded by two copies of IS*26* and flanked by 8 bp target site duplications.

Plasmid conjugation into *P. mirabilis*

Variants of pOXA-48 were conjugated from seven Enterobacterales isolates (*K. pneumoniae, E. coli,* and *Citrobacter freundii*) in parallel to the recipients *P. mirabilis* ARP and *E. coli* J53. Some of the donor isolates have been characterized previously (KP17051, EC8448 [11], EC7215 [33]). In 6/7 isolates, transconjugants of both recipients harboured intact pOXA-48-like plasmids and no other plasmids. In one ARP transconjugant, Tc-KP17051-ARP, genomic analysis revealed a truncated bla_{OXA-48}-carrying plasmid of 18 kb size in the initial conjugation experiment, but the plasmid remained intact during transfer in follow-up experiments. Hence, this isolate pair was excluded from the comparative MIC analysis. For the other six transconjugant pairs, MICs for PIT and ertapenem were significantly lower in ARP transconjugants than in J53 transconjugants, while they were on a comparable level for meropenem (Figure 7, Supplementary Table 3). The pOXA-48 conjugation rates to J53 and ARP were compared from two

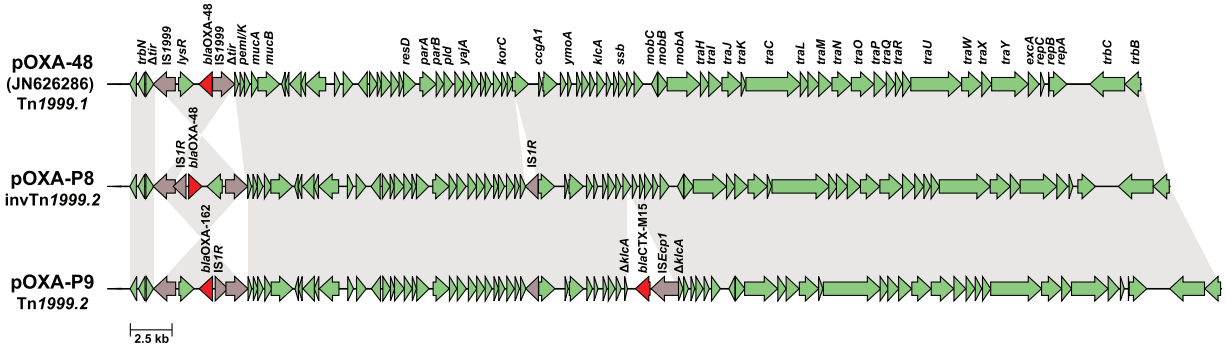

Figure 4. Plasmid variants of pOXA-48 found in two *P. mirabilis* isolates. Grey arrows = mobile genetic elements, red arrows = antibiotic resistance genes, green arrows = other genes or open reading frames. Unlabelled arrows indicate genes coding for hypothetical proteins.

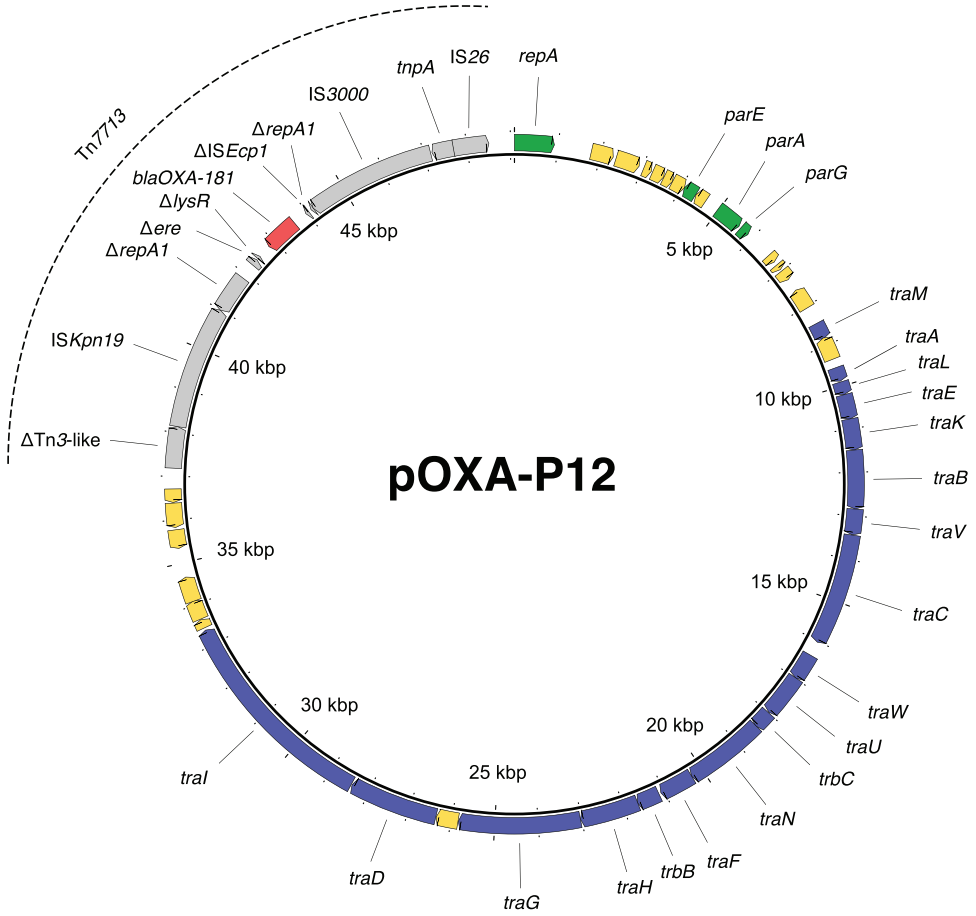

Figure 5. The novel MOB$_F$ plasmid pOXA-P12, harbouring *bla*$_{OXA-181}$ within the novel transposon Tn*7713*. Red arrow = *bla*$_{OXA-48}$, grey arrows = other parts of Tn*7713*, green arrows = genes associated with plasmid replication, blue arrows = genes associated with plasmid transfer, yellow arrows = genes coding for hypothetical proteins.

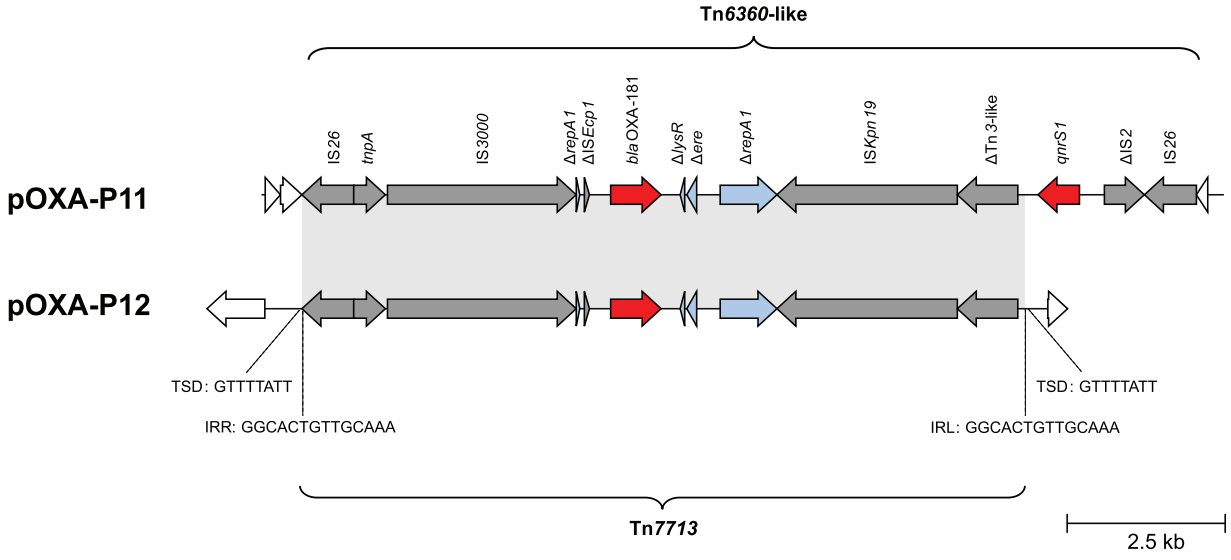

Figure 6. Tn*6360*-like variants in *bla*$_{OXA-181}$-harbouring *P. mirabilis*. Grey arrows = mobile genetic elements or associated genes, red arrows = antibiotic resistance genes, blue arrows = other genes or gene fragments, white arrows = genes outside of the transposon structure. IRL/IRR = left and right inverted repeats, TSD = target site duplications.

representative donors, *E. coli* EC7215 and *K. pneumoniae* KP12369. They were significantly higher when transferred into J53 (3.59×10^{-4} [SD 1.37×10^{-4}] and 1.7×10^{-3} [SD 2×10^{-3}]) than into ARP (1.39×10^{-6} [SD 1.39×10^{-6}] and 4.94×10^{-7} [SD 1.86×10^{-7}]).

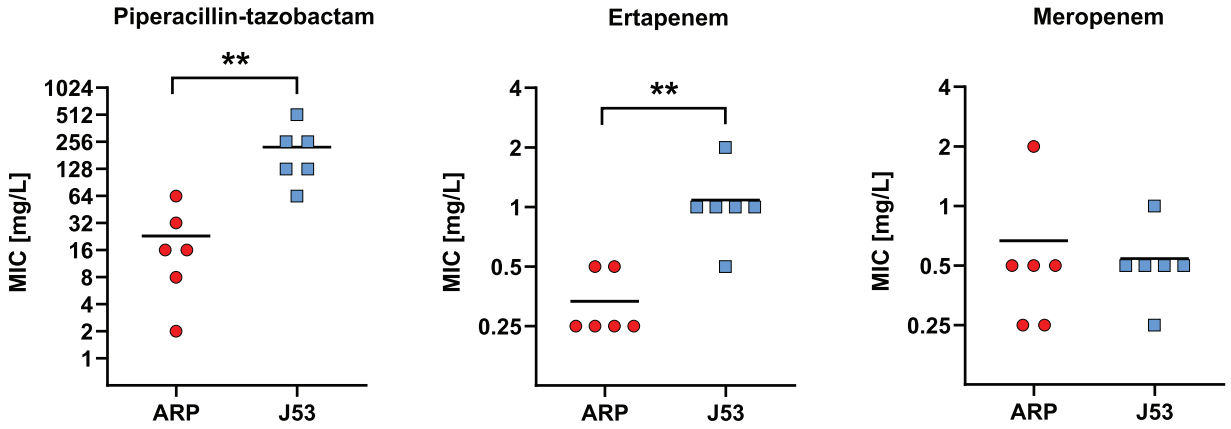

Figure 7. Minimal inhibitory concentrations (MICs) of piperacillin-tazobactam, ertapenem and meropenem for OXA-48-producing transconjugants. Transconjugants comprise *P. mirabilis* ARP (red dots, $n = 6$) and *E. coli* J53 (blue squares, $n = 6$), sharing isogenic pOXA-48-like plasmid variants. Black bars indicate the median. Two asterisks indicate a statistically significant difference of $p \leq 0.01$.

Discussion

In this study, we characterized $bla_{\text{OXA-48}}$-like-producing *P. mirabilis* and reported on so far undescribed plasmids and transposons.

High ratio of chromosomal $bla_{\text{OXA-48}}$ integration

With 7/9 OXA-48-producing isolates, this study demonstrated a high rate of chromosomally integrated $bla_{\text{OXA-48}}$ in *P. mirabilis* compared to other Enterobacterales [33]. Only in one isolate, $bla_{\text{OXA-48}}$ had the typical genomic location within a Tn*1999*-like transposon on an IncL plasmid, which is usually present in *K. pneumoniae* or *E. coli*. From the scarce available data on $bla_{\text{OXA-48}}$ in *P. mirabilis*, two studies found $bla_{\text{OXA-48}}$ located on IncL/M plasmids [12,34], while a third study detected $bla_{\text{OXA-48}}$ on the chromosome of a *P. mirabilis* outbreak clone in Spain [4].

Our results might indicate, that the genetic environment of *P. mirabilis* is highly supportive for chromosomal integration of $bla_{\text{OXA-48}}$.

First, based on our data and the studies mentioned above, invTn*1999.2* seems to be the exclusive Tn*1999* variant in $bla_{\text{OXA-48}}$-carrying *P. mirabilis* isolates. This is in contrast to other Enterobacterales, where Tn*1999.2* and Tn*1999.1* prevail [33]. This can explain the high ratio of chromosomal insertion via Tn*6237* in *P. mirabilis,* where invTn*1999.2* leads to a configuration that allows for pseudo-compound transposition of the $bla_{\text{OXA-48}}$ environment via two copies of IS*1R*. While this is only occasionally described in other Enterobacterales, mainly in *E. coli* ST38 [35], this was observed at a high ratio ($n = 3$) in this study. As the respective isolates are phylogenetically distant and the insertions sites of Tn*6237* differs between isolates, this indicates several integration events instead of clonal spread.

Second, *P. mirabilis* strains contain genomic islands at high frequency, e.g. of the type SGI1[36], PGI1 [37], PGI2 [38], GIPmi1 [39] or PmGRI1 [28]. These genomic islands, including the novel PmGRI1 variants described in this study, are rich in mobile genetic elements, such as transposons and insertion sequences, making them a potential hot spot for the integration of foreign genome sequences. The integration of DNA segments containing resistance genes in the chromosome via homologous recombination has been reported, e.g. for *Acinetobacter baumannii* [40] and subsequent integration events can lead to Russian doll-like structured genomic islands in this species [41]. Our study suggests a similar genomic island evolution for *P. mirabilis*, as illustrated in Figure 3, where some PmGRI1 variants might have evolved from each other and other genomic structures. Furthermore, novel variants of PmGRI1 with different genetic content have been described recently, indicating an ongoing evolution. Isolates harbouring these PmGRI1 variants were obtained from human samples [42,43], swine [44], and chicken [28]. This emphasizes the important link of *P. mirabilis* for the spread of multidrug resistance between animals and humans, as highlighted in previous studies [45].

Another possible explanation for the high rate of chromosomal integration of $bla_{\text{OXA-48}}$ in *P. mirabilis* would be that the $bla_{\text{OXA-48}}$-carrying plasmids are unstable in this species, therefore selecting for isolates with chromosomal location. This hypothesis has not been tested in this study, which is a limitation.

Genomic environments of $bla_{\text{OXA-181}}$ in P. mirabilis

The presence of a $bla_{\text{OXA-181}}$-carrying IncX3 plasmid in *P. mirabilis* identical to one described in *E. coli* before [31], as well as a large number of plasmid

sequence matches in other Enterobacterales species on GenBank, indicates interspecies spread which could also be shown *in vitro* in this study. Possibly $bla_{OXA-181}$ was transferred from the IncX3 plasmid to the MOB_F plasmid, pOXA-P12, via Tn*7713*. This plasmid was also capable of interspecies conjugation *in vitro*. The plasmid pOXA-P12 was detected in two isolates, which were isolated with a time difference of 2.5 years and had no spatial relationship. This could indicate either repeated integration events or high stability of this plasmid in *P. mirabilis*. Interestingly, the initially described $bla_{OXA-181}$-carrying ColE2 plasmid (synonym: ColKP3) was not self-conjugative, at least *in vitro* [46]. However, after mobilization of the genetic environment onto the IncX3 plasmid it could conjugate to *E. coli* J53 and *K. pneumoniae* PRZ *in vitro* in the absence of other plasmids. Mobilization of $bla_{OXA-181}$ onto self-transmissible plasmids could be an alarming event, as this could support the hypothesis of a silent spread of bla_{OXA-48}-like through *P. mirabilis*.

Low MICs for carbapenems and piperacillin-tazobactam

Carbapenem and PIT MICs were unevenly distributed among the clinical isolates. As 10/13 isolates exhibit only slightly elevated carbapenem MICs (0.25–1 mg/L), the presence of OXA-48-like might be missed in the diagnostic laboratory, depending on the screening algorithm used.

MICs for PIT are usually strongly elevated in OXA-48-like-producing Enterobacterales, typically >128 mg/L [47]. In this study, three isolates exhibited PIT MICs in the susceptible range, all of which harboured bla_{OXA-48} on their chromosome. This finding could indicate an association between the chromosomal location of bla_{OXA-48} and low PIT MICs. Low PIT MIC could be mediated by lower copy numbers of chromosomal bla_{OXA-48} compared to plasmidic location, which is supported by the relative contig depth estimation of Unicycler in 5/6 bla_{OXA-48}-like-harbouring plasmids (Supplementary Table 4). However, susceptibility to PIT could not be solely inferred from chromosomal location even in the absence of other β-lactamase genes (e.g. P5 and P7). Furthermore, conjugation experiments showed that the presence of a pOXA-48 variant in a *P. mirabilis* recipient also led to PIT MICs in the susceptible range in some isolates, indicating that PIT susceptibility is not strictly associated with chromosomal location. A mutation in the bla_{OXA-48} promoter region can be a reason for PIT susceptibility in OXA-48-producing *P. mirabilis* [4]; however, this was ruled out in our isolates. Overall, these data indicate that in *P. mirabilis* the susceptibility phenotype for carbapenems and PIT might be influenced by non-enzymatic resistance mechanisms, of which, for example, alterations of the penicillin-binding proteins as well as outer membrane proteins have been described [48,49], which should be analysed in future studies.

Interspecies conjugation of bla_{OXA-48}-like-carrying plasmids

While interspecies conjugation of the highly conjugative pOXA-48-like plasmids in other bla_{OXA-48}-carrying Enterobacterales has been described as a main mediator for the spread of OXA-48 [33,50], this has not been comprehensively studied in *P. mirabilis*.

This study showed interspecies conjugation of bla_{OXA-48}-carrying plasmids in both directions; from *P. mirabilis* into *E. coli* and from different Enterobacterales species into *P. mirabilis*. Conjugation of other carbapenemase-carrying plasmids from *E. coli* to *P. mirabilis* (reference strain CIP103181) has been described before at low transfer frequencies compared to other Enterobacterales recipients [51]. However, this is to the best of our knowledge the first description of conjugation of the widespread pOXA-48-like plasmids to *P. mirabilis*. These data indicate that *P. mirabilis* participates in the spread of bla_{OXA-48}-like-carrying plasmids between Enterobacterales *in vivo*. In combination with a difficult-to-detect resistance phenotype, this could be an alarming finding, as bla_{OXA-48}-like-carrying mobile genetic elements could be distributed within the Enterobacterales communities below the radar of surveillance. However, to estimate the burden of *P. mirabilis* in the spread of OXA-48-like, reliable detection methods need to be implemented first in diagnostic laboratories. An algorithm with 100% sensitivity in the detection of carbapenemase-producing *P. mirabilis* has been described recently and implementation might be advocated in the face of the results of this study [5].

Limitations

A limitation of this study is that it only comprises isolates from Germany and Austria. The genetic environment of bla_{OXA-48}-like in *P. mirabilis* seems to be diverse, and the genetic background of the included isolates differs from the isolates published so far from other countries. Furthermore, other OXA-48-like subtypes have been described in *P. mirabilis* from other countries, such as OXA-204 in France [52] and OXA-244 in Russia [34]. Therefore, it is likely that in other geographic regions, different genetic environments of bla_{OXA-48}-like are present, which should be further studied.

Another limitation is that the species-specific factors contributing to different MICs in different species with an isogenic plasmid that were observed in this study have not been further investigated.

Conclusion

This study showed that the genetic environments of bla_{OXA-48}-like in *P. mirabilis* are essentially different from those seen in other Enterobacterales, but bla_{OXA-48}-like can be transferred between *P. mirabilis* and other Enterobacterales by various mobile genetic elements. Together with a hard-to-detect phenotype, *P. mirabilis* therefore likely contributes to the global spread of OXA-48-like enzymes in Enterobacterales.

Disclosure statement

No potential conflict of interest was reported by the author(s).

Funding

This study was supported by the Koeln Fortune Program and Maria-Pesch-Foundation/Faculty of Medicine, University of Cologne; Forschungspool of the University of Oldenburg; German Center for Infection Research under grant TTU 08.923_00; Scholarship by the Deutsche Forschungsgemeinschaft (German Research Foundation, project no. 493624332), Dr. Rolf M. Schwiete-Stiftung; and the Federal Ministry of Education and Research under grant BMBF 16LW0392.

ORCID

Janko Sattler http://orcid.org/0000-0003-1415-4169
Janina Noster http://orcid.org/0000-0002-8802-6605
Kyriaki Xanthopoulou http://orcid.org/0000-0001-8591-8184
Julian Sommer http://orcid.org/0009-0006-3654-2006
Stephan Göttig http://orcid.org/0000-0001-6896-5309
Axel Hamprecht http://orcid.org/0000-0003-1449-5780

References

[1] Nordmann P, Poirel L. The difficult-to-control spread of carbapenemase producers among *Enterobacteriaceae* worldwide. Clin Microbiol Infect. 2014;20:821–830. doi:10.1111/1469-0691.12719

[2] Potron A, Poirel L, Rondinaud E, et al. Intercontinental spread of OXA-48 beta-lactamase-producing Enterobacteriaceae over a 11-year period, 2001 to 2011. Eurosurveillance. 2013;18:20549. doi:10.2807/1560-7917.ES2013.18.31.20549

[3] Girlich D, Bonnin RA, Dortet L, et al. Genetics of Acquired Antibiotic Resistance Genes in *Proteus* spp. Front Microbiol. 2020;11:256. doi:10.3389/fmicb.2020.00256

[4] Pedraza R, Kieffer N, Guzmán-Puche J, et al. Hidden dissemination of carbapenem-susceptible OXA-48-producing *Proteus mirabilis*. J Antimicrob Chemother. 2022;77:3009–3015. doi:10.1093/jac/dkac267

[5] Hamprecht A, Sattler J, Noster J, et al. *Proteus mirabilis* – analysis of a concealed source of carbapenemases and development of a diagnostic algorithm for detection. Clin Microbiol Infect. 2023;29:1198.e1–1198.e6. doi:10.1016/j.cmi.2023.05.032

[6] European Committee on Antimicrobial Susceptibility Testing. EUCAST guidelines for detection of resistance mechanisms and specific resistances of clinical and/or epidemiological importance. Version 2.0. July 2017. Available from: https://www.eucast.org/resistance_mechanisms

[7] Huang T-D, Poirel L, Bogaerts P, et al. Temocillin and piperacillin/tazobactam resistance by disc diffusion as antimicrobial surrogate markers for the detection of carbapenemase-producing Enterobacteriaceae in geographical areas with a high prevalence of OXA-48 producers. J Antimicrob Chemother. 2014;69:445–450. doi:10.1093/jac/dkt367

[8] Wiskirchen DE, Nordmann P, Crandon JL, et al. Efficacy of humanized carbapenem and ceftazidime regimens against *Enterobacteriaceae* producing OXA-48 carbapenemase in a murine infection model. Antimicrob Agents Chemother. 2014;58:1678–1683. doi:10.1128/AAC.01947-13

[9] Skalova A, Chudejova K, Rotova V, et al. Molecular characterization of OXA-48-like-producing Enterobacteriaceae in the Czech Republic and evidence for horizontal transfer of pOXA-48-like plasmids. Antimicrob Agents Chemother. 2017;61:e01889–16. doi:10.1128/AAC.01889-16

[10] Carrër A, Poirel L, Eraksoy H, et al. Spread of OXA-48-positive carbapenem-resistant *Klebsiella pneumoniae* isolates in Istanbul, Turkey. Antimicrob Agents Chemother. 2008;52:2950–2954. doi:10.1128/AAC.01672-07

[11] Sattler J, Tsvetkov T, Stelzer Y, et al. Emergence of Tn*1999.7*, a new transposon in blaOXA-48-harboring plasmids associated with increased plasmid stability. Antimicrob Agents Chemother. 2022;0:e00787–22.

[12] Chen L, Laham A, Chavda N, et al. First report of an OXA-48-producing multidrug-resistant *Proteus mirabilis* strain from Gaza, Palestine. Antimicrob Agents Chemother; 2015; 59:4305–4307. doi:10.1128/AAC.00565-15

[13] Greissl C, Saleh A, Hamprecht A. Rapid detection of OXA-48-like, KPC, NDM, and VIM carbapenemases in Enterobacterales by a new multiplex immunochromatographic test. Eur J Clin Microbiol Infect Dis. 2019;38:331–335. doi:10.1007/s10096-018-3432-2

[14] Baeza LL, Pfennigwerth N, Greissl C, et al. Comparison of five methods for detection of carbapenemases in Enterobacterales with proposal of a new algorithm. Clin Microbiol Infect. 2019;25:1286.e9–1286.e15. doi:10.1016/j.cmi.2019.03.003

[15] Wick RR, Judd LM, Cerdeira LT, et al. Trycycler: consensus long-read assemblies for bacterial genomes. Genome Biol. 2021;22:266. doi:10.1186/s13059-021-02483-z

[16] Wright C, Wykes M. nanoporetech/medaka [Internet]. Oxford Nanopore Technologies; 2024 [cited 2024 Mar 8]. Available from: https://github.com/nanoporetech/medaka

[17] Wick RR, Holt KE. Polypolish: Short-read polishing of long-read bacterial genome assemblies. PLOS Comput Biol. 2022;18:e1009802. doi:10.1371/journal.pcbi.1009802

[18] Zankari E, Hasman H, Cosentino S, et al. Identification of acquired antimicrobial resistance genes. J Antimicrob Chemother. 2012;67:2640–2644. doi:10.1093/jac/dks261

[19] Carattoli A, Zankari E, García-Fernández A, et al. *In silico* detection and typing of plasmids using

PlasmidFinder and plasmid multilocus sequence typing. Antimicrob Agents Chemother. 2014;58:3895–3903. doi:10.1128/AAC.02412-14

[20] Garcillán-Barcia MP, Redondo-Salvo S, Vielva L, et al. Mobscan: automated annotation of MOB Relaxases. Methods Mol Biol Clifton NJ. 2020;2075:295–308. doi:10.1007/978-1-4939-9877-7_21

[21] Robertson J, Nash JHE. MOB-suite: software tools for clustering, reconstruction and typing of plasmids from draft assemblies. Microb Genomics. 2018;4:e000206.

[22] Tatusova T, DiCuccio M, Badretdin A, et al. NCBI prokaryotic genome annotation pipeline. Nucleic Acids Res. 2016;44:6614–6624. doi:10.1093/nar/gkw569

[23] Silva M, Machado MP, Silva DN, et al. chewBBACA: a complete suite for gene-by-gene schema creation and strain identification. Microb Genomics. 2018;4:e000166. doi:10.1099/mgen.0.000166

[24] Zhou Z, Alikhan N-F, Sergeant MJ, et al. GrapeTree: visualization of core genomic relationships among 100,000 bacterial pathogens. Genome Res. 2018;28:1395–1404. doi:10.1101/gr.232397.117

[25] Kaas RS, Leekitcharoenphon P, Aarestrup FM, et al. Solving the problem of comparing whole bacterial genomes across different sequencing platforms. PLoS One. 2014;9:e104984. doi:10.1371/journal.pone.0104984

[26] Alikhan N-F, Petty NK, Ben Zakour NL, et al. BLAST Ring Image Generator (BRIG): simple prokaryote genome comparisons. BMC Genomics. 2011;12:402. doi:10.1186/1471-2164-12-402

[27] Gilchrist CLM, Chooi Y-H. Clinker & clustermap.js: automatic generation of gene cluster comparison figures. Bioinformatics. 2021;37:2473–2475. doi:10.1093/bioinformatics/btab007

[28] Lei C-W, Yao T-G, Yan J, et al. Identification of *Proteus* genomic island 2 variants in two clonal *Proteus mirabilis* isolates with coexistence of a novel genomic resistance island PmGRI1. J Antimicrob Chemother. 2020;75:2503–2507. doi:10.1093/jac/dkaa215

[29] Hua X, Zhang L, Moran RA, et al. Cointegration as a mechanism for the evolution of a KPC-producing multidrug resistance plasmid in *Proteus mirabilis*. Emerg Microbes Infect. 2020;9:1206–1218. doi:10.1080/22221751.2020.1773322

[30] Alvarez-Fraga L, Phan M-D, Goh KGK, et al. Differential Afa/Dr fimbriae expression in the multidrug-resistant *Escherichia coli* ST131 clone. mBio. 2022;13:e03519–21. doi:10.1128/mbio.03519-21

[31] Liu Y, Feng Y, Wu W, et al. First report of OXA-181-producing *Escherichia coli* in China and characterization of the isolate using whole-genome sequencing. Antimicrob Agents Chemother. 2015;59:5022–5025. doi:10.1128/AAC.00442-15

[32] Tansirichaiya S, MdA R, Roberts AP. The transposon registry. Mob DNA. 2019;10:40. doi:10.1186/s13100-019-0182-3

[33] Hamprecht A, Sommer J, Willmann M, et al. Pathogenicity of clinical OXA-48 isolates and impact of the OXA-48 IncL plasmid on virulence and bacterial fitness. Front Microbiol. 2019;10:2509. doi:10.3389/fmicb.2019.02509

[34] Fursova NK, Astashkin EI, Knyazeva AI, et al. The spread of bla_{OXA-48} and $bla_{OXA-244}$ carbapenemase genes among *Klebsiella pneumoniae*, *Proteus mirabilis* and *Enterobacter* spp. isolated in Moscow, Russia. Ann Clin Microbiol Antimicrob. 2015;14:46. doi:10.1186/s12941-015-0108-y

[35] Beyrouthy R, Robin F, Delmas J, et al. IS*1R*-mediated plasticity of IncL/M plasmids leads to the insertion of bla_{OXA-48} into the *Escherichia coli* chromosome. Antimicrob Agents Chemother. 2014;58:3785–3790. doi:10.1128/AAC.02669-14

[36] Ahmed AM, Hussein AIA, Shimamoto T. *Proteus mirabilis* clinical isolate harbouring a new variant of *Salmonella* genomic island 1 containing the multiple antibiotic resistance region. J Antimicrob Chemother. 2007;59:184–190. doi:10.1093/jac/dkl471

[37] Siebor E, Neuwirth C. *Proteus* genomic island 1 (PGI1), a new resistance genomic island from two *Proteus mirabilis* French clinical isolates. J Antimicrob Chemother. 2014;69:3216–3220. doi:10.1093/jac/dku314

[38] Lei C-W, Chen Y-P, Kong L-H, et al. PGI2 is a novel SGI1-relative multidrug-resistant genomic island characterized in *Proteus mirabilis*. Antimicrob Agents Chemother. 2018;62. doi:10.1128/aac.00019-18

[39] Siebor E, de Curraize C, Neuwirth C. Genomic context of resistance genes within a French clinical MDR *Proteus mirabilis*: identification of the novel genomic resistance island GI*Pmi*1. J Antimicrob Chemother. 2018;73:1808–1811. doi:10.1093/jac/dky126

[40] Hamidian M, Hawkey J, Wick R, et al. Evolution of a clade of *Acinetobacter baumannii* global clone 1, lineage 1 via acquisition of carbapenem- and aminoglycoside-resistance genes and dispersion of ISAba1. Microb Genomics. 2019;5:e000242.

[41] Hua X, Moran RA, Xu Q, et al. Acquisition of a genomic resistance island (AbGRI5) from global clone 2 through homologous recombination in a clinical *Acinetobacter baumannii* isolate. J Antimicrob Chemother. 2021;76:65–69. doi:10.1093/jac/dkaa389

[42] Pilato D, Chiarelli V, Boinett A, et al. Complete genome sequence of the first KPC-type carbapenemase-positive *Proteus mirabilis* strain from a bloodstream infection. Genome Announc. 2016;4. doi:10.1128/genomeA.00607-16

[43] Li Y, Liu Q, Qiu Y, et al. Genomic characteristics of clinical multidrug-resistant *Proteus* isolates from a tertiary care hospital in southwest China. Front Microbiol. 2022;13:977356. doi:10.3389/fmicb.2022.977356

[44] He J, Lei C, Li C, et al. Identification of a novel genomic resistance island PmGRI1-STP3 and an SXT/R391 integrative conjugative element in *Proteus mirabilis* of swine origin in China. J Glob Antimicrob Resist. 2021;25:77–81. doi:10.1016/j.jgar.2021.02.018

[45] Schultz E, Haenni M, Mereghetti L, et al. Survey of multidrug resistance integrative mobilizable elements SGI1 and PGI1 in *Proteus mirabilis* in humans and dogs in France, 2010–13. J Antimicrob Chemother. 2015;70:2543–2546. doi:10.1093/jac/dkv154

[46] Potron A, Nordmann P, Lafeuille E, et al. Characterization of OXA-181, a carbapenem-hydrolyzing class D β-lactamase from *Klebsiella pneumoniae*. Antimicrob Agents Chemother. 2011;55:4896–4899. doi:10.1128/AAC.00481-11

[47] Tsakris A, Poulou A, Bogaerts P, et al. Evaluation of a new phenotypic OXA-48 disk test for differentiation of OXA-48 carbapenemase-producing *Enterobacteriaceae* clinical isolates. J Clin Microbiol. 2015;53:1245–1251. doi:10.1128/JCM.03318-14

[48] Neuwirth C, Siébor E, Duez J-M, et al. Imipenem resistance in clinical isolates of *Proteus mirabilis*

associated with alterations in penicillin-binding proteins. J Antimicrob Chemother. 1995;36:335–342. doi:10.1093/jac/36.2.335

[49] Tsai Y-L, Wang M-C, Hsueh P-R, et al. Overexpression of an outer membrane protein associated with decreased susceptibility to carbapenems in *Proteus mirabilis*. PLoS One. 2015;10: e0120395.

[50] Sommer J, Gerbracht KM, Krause FF, et al. OXA-484, an OXA-48-type carbapenem-hydrolyzing class D β-lactamase from *Escherichia coli*. Front Microbiol. 2021;12:660094–660094. doi:10.3389/fmicb.2021.660094

[51] Potron A, Poirel L, Nordmann P. Plasmid-mediated transfer of the $bla_{\text{NDM-1}}$ gene in Gram-negative rods. FEMS Microbiol Lett. 2011;324:111–116. doi:10.1111/j.1574-6968.2011.02392.x

[52] Potron A, Bernabeu S, Cuzon G, et al. Analysis of OXA-204 carbapenemase-producing *Enterobacteriaceae* reveals possible endoscopy-associated transmission, France, 2012 to 2014. Eurosurveillance. 2017;22:17. doi:10.2807/1560-7917.ES.2017.22.49.17-00048